

Estimation of the stiffness tensor of dry rock core sample through numerical simulations based on rock physics

Juan E. Santos * School of Earth Sciences and Engineering, Hohai University, Universidad de Buenos Aires, Facultad de Ingeniería, Instituto del Gas y del Petróleo, Department of Mathematics, Purdue University, A. Sanchez Camus, Facultad de Ciencias Astronómicas y Geofísicas, Universidad Nacional de La Plata, Gabriela B. Savioli, Universidad de Buenos Aires, Facultad de Ingeniería, Instituto del Gas y del Petróleo, Patricia M. Gauzellino, Facultad de Ciencias Astronómicas y Geofísicas, Universidad Nacional de La Plata, Jing Ba, School of Earth Sciences and Engineering, Hohai University

SUMMARY

From a mechanical perspective, organic mudrocks are viscoelastic media whose anisotropy can be accurately represented using a vertical transverse isotropy (VTI) model. These reservoirs exhibit ultra-low permeability, typically in the range of nano to microdarcies, and possess a complex pore structure. Such characteristics, along with different oil, gas and water fluids saturations, significantly impact the hydraulic properties and mechanical behavior of the reservoir during production. This study introduces a practical methodology to estimate the stiffness tensor of dry rock using theoretical models of rock physics, incorporating mechanical, mineralogical, and petrophysical data from a core extracted from the lower section of the Vaca Muerta Formation, located in the Neuquén Basin, Argentina. This core was extracted from a block located in the maximum oil generation window of the Vaca Muerta formation at a depth of 3100 m. After determining the dry-rock stiffness tensor, the proposed methodology enables to analyze the effects caused by fluid saturation and seismic source frequencies, ranging from laboratory experiments and well logging to field seismic studies. Numerical results exhibit excellent agreement with laboratory phase velocities measured at 1 MHz, with errors below 5 %. The procedure is then validated as an effective tool for evaluating critical phenomena such as attenuation and dispersion caused by wave-induced fluid flow (WIFF). Once the model parameters have been calibrated, the stiffness tensor can be extrapolated to other areas within the block using only mineralogical and petrophysical information (porosity and permeability). This significantly simplifies the geomechanical and seismic characterization of unconventional reservoirs.

THEORY FOR VTI MEDIA

The Vaca Muerta formation consists of a sequence of very thin layers which at long wavelengths compared with the average layer thickness behaves as a transversely isotropic anisotropy with a vertical axis - VTI (?), although it may change its elastic symmetry due to the presence of fractures. A VTI medium is characterized by five independent elastic moduli $c_{11}, c_{13}, c_{33}, c_{55}, c_{66}$. In this case, the stress-strain relationship

in Voigt notation is given by (Tsvankin et al, 2001).

$$\begin{bmatrix} \sigma_{11} \\ \sigma_{22} \\ \sigma_{33} \\ \sigma_{23} \\ \sigma_{31} \\ \sigma_{12} \end{bmatrix} = \begin{bmatrix} c_{11} & c_{12} & c_{13} & 0 & 0 & 0 \\ c_{12} & c_{11} & c_{13} & 0 & 0 & 0 \\ c_{13} & c_{13} & c_{33} & 0 & 0 & 0 \\ 0 & 0 & 0 & c_{55} & 0 & 0 \\ 0 & 0 & 0 & 0 & c_{55} & 0 \\ 0 & 0 & 0 & 0 & 0 & c_{66} \end{bmatrix} \cdot \begin{bmatrix} \epsilon_{11} \\ \epsilon_{22} \\ \epsilon_{33} \\ 2\epsilon_{23} \\ 2\epsilon_{31} \\ 2\epsilon_{12} \end{bmatrix} \quad (1)$$

with the vectors σ and ϵ being the stress and the strain, respectively, and $c_{12} = c_{11} - 2c_{66}$

Attenuation and dispersion of the material can be represented through an equivalent viscoelastic medium, characterized by complex and frequency dependent stiffness p_{ij} , with the imaginary part representing attenuation. Therefore, with $\tilde{\sigma}$ and $\tilde{\epsilon}$ denote the stress and strain of the equivalent viscoelastic VTI medium we have the relations

$$\begin{bmatrix} \tilde{\sigma}_{11} \\ \tilde{\sigma}_{22} \\ \tilde{\sigma}_{33} \\ \tilde{\sigma}_{23} \\ \tilde{\sigma}_{31} \\ \tilde{\sigma}_{12} \end{bmatrix} = \begin{bmatrix} p_{11} & p_{12} & p_{13} & 0 & 0 & 0 \\ p_{12} & p_{11} & p_{13} & 0 & 0 & 0 \\ p_{13} & p_{13} & p_{33} & 0 & 0 & 0 \\ 0 & 0 & 0 & p_{55} & 0 & 0 \\ 0 & 0 & 0 & 0 & p_{55} & 0 \\ 0 & 0 & 0 & 0 & 0 & p_{66} \end{bmatrix} \cdot \begin{bmatrix} \tilde{\epsilon}_{11} \\ \tilde{\epsilon}_{22} \\ \tilde{\epsilon}_{33} \\ 2\tilde{\epsilon}_{23} \\ 2\tilde{\epsilon}_{31} \\ 2\tilde{\epsilon}_{12} \end{bmatrix} \quad (2)$$

where $p_{12} = p_{11} - 2p_{66}$.

White et al (1975) described the equivalent viscoelastic medium of a periodic sequence of alternating thin layers of thickness d_1 and d_2 , with symmetry axes normal to the layering plane. Their theory gives the complex and frequency dependent stiffness p_{33} , as:

$$p_{33} = \left[\frac{1}{c_{33}} + \frac{2(r_2 - r_1)^2}{i\omega(d_1 + d_2)(I_1 + I_2)} \right]^{-1}, \quad (3)$$

where

$$r = \frac{\alpha M}{E_G}, I = \frac{\eta}{\kappa a} \coth\left(\frac{ad}{2}\right), a = \sqrt{\frac{i\omega\eta E_G}{\kappa M E_m}} \quad (4)$$

for each single layer. In Eq.(4), $\alpha = 1 - \frac{K_m}{K_s}$, $E_G = E_m + \alpha^2 M$,

$E_m = K_m + \frac{4}{3}\mu$, $M = \left[\frac{\alpha - \phi}{K_s} + \frac{\phi}{K_f} \right]^{-1}$, with K_s , K_m and K_f

the solid grains, dry matrix and saturant fluid bulk moduli; μ is the shear modulus, η is the fluid viscosity, κ is the permeability, ϕ the porosity, ω the frequency and i the imaginary unit.

Estimation of the stiffness tensor of dry rock core sample through numerical simulations based on rock physics

Gelinsky and Shapiro (3) determined the relaxed and unrelaxed stiffnesses of the equivalent poro-viscoelastic medium to a periodic sequence of finely layered horizontally homogeneous material, while Krzikalla and Müller (6) combined the two previous models, i.e., they computed p_{33} as in Eq.(3) and obtained the other five stiffnesses of the equivalent TIV medium as,

$$p_{ij}(\omega) = c_{ij} + \left(\frac{c_{ij} - c_{ij}^r}{c_{33} - c_{33}^r} \right) [p_{33}(\omega) - c_{33}], \quad (5)$$

where c_{ij}^r are the relaxed stiffnesses, computed as shown in the Appendix (Gelinsky and Shapiro, 1997). The main assumption in Eq. (5) is that the fluid-flow direction is perpendicular to the layering so that the relaxation behavior is described by a single stiffness, $p_{33}(\omega)$ (Krzikalla and Müller, 2011). Thus the theory is not valid when the layers are heterogeneous.

Velocity and quality factor of the qP, qS and SH waves for the equivalent anisotropic medium were computed from the complex velocities (see (Carcione, 2007)).

RESULTS

Data

A dry core from the Vaca Muerta Formation is the source of the measured data, which consist of rock mineralogy and phase velocities, vp_{11} , vp_{33} , vp_{55} and vp_{66} of the dry core at 3100 m depth. This core corresponds to the window of maximum oil generation in the formation (see Figure 1).

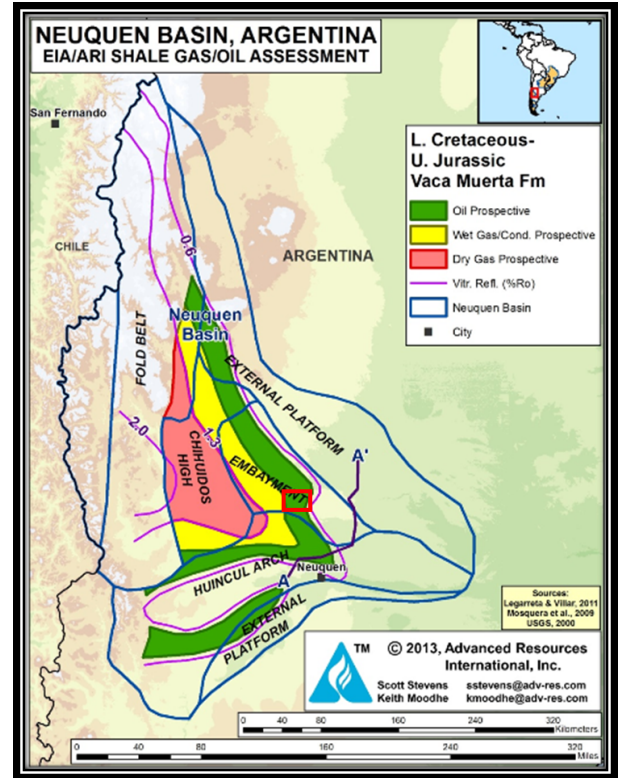


Figure 1: The green region corresponds to the the oil-generating window in the Vaca Muerta formation.

Estimation of the stiffness tensor of dry rock core sample through numerical simulations based on rock physics

The objective of this study is to verify that by knowing the mineralogy and applying theoretical models of rock physics, we are able to obtain accurate estimate the elastic tensor coefficients p_{ij} .

The numerical experiments consider an alternating periodic sequence of 1 mm thickness. Each period consists of eighty layers, seventy nine layers of Material 1 and one layer of Material 2.

Material 1 is composed of seven minerals, including 23 % kerogen, 37.27 % Clay, 14.61 % Quartz, 10.68 % Calcite, 2.57 % Plagioclase, 2.37 % Dolomite and 3.5 % Pyrite. Using the solid grains density, bulk and shear moduli of each mineral and a generalized Krief model (see Carcione et al, 2005), we obtained the values K_s , K_m , μ_m for the dry core as shown in Table 1. We also computed the average density of Material 1. Besides, the single layer of Material 2 consists of dry kerogen. Its properties can be seen in Table 1. Both materials have 6 % porosity and $2.75 \cdot 10^{-18} \text{ m}^2$ permeability.

Table 1. Properties of Materials

Property	Material 1 (Composite)	Material 2 (kerogen)
K_s (GPa)	34.34	7.0
K_m (GPa)	29.19	1.29
μ_m (GPa)	15.69	0.36
ρ (kg/m ³)	2487	1400

Computed VTI phase velocities using the dry-core data

We compute the numerical stiffness coefficients p_{ij} applying the methodology described in section "Mesoscopic-flow attenuation theory for VTI media" and the data of Table 1. We consider a 1 mm thickness periodic sequence, each period having seventy nine layers of Material 1 and one layer of Material 2. The mesh size is $1.25 \cdot 10^{-5} \text{ mm}$, then the sizes of layers 1 and 2 are $9.875 \cdot 10^{-4} \text{ mm}$ and $1.25 \cdot 10^{-5} \text{ mm}$, respectively. Since the phase velocity data corresponds to a dry sample, the numerical experiment consider air as the saturating fluid. Table 2 summarizes the results of the VTI experiments.

Table 2. Phase velocities from the numerical experiments, the measured ones and error percentage. Frequency is 1 MHz

Phase velocity (m/s)	Computed	Measured	error (%)
v_{p11}	4538.29	4331	4.79 %
v_{p33}	4008.93	4217.47	4.96 %
v_{p55}	2098.69	2193.61	4.33 %
v_{p66}	2581.97	2464	4.79 %

In all computed velocities the error of less than 5% was obtained, which is considered a very good match since it is within the range of measurement errors. Hence we can then rely on the numerically estimated values of the stiffness coefficients p_{ij} shown in Table 3.

Table 3. Numerical p_{ij} values from the VTI experiments (Pa). Frequency is 1 MHz

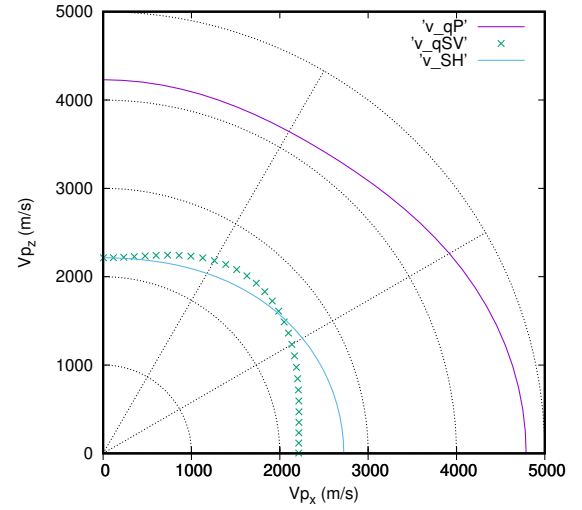


Figure 2: Polar representation of phase velocities of qP, qSV and SH waves at 1 MHz. The medium consists of a periodic sequence of seventy nine dry layers of the composite porous solid including kerogen as a mineral with 23 % proportion, and one dry kerogen layer. Thus kerogen content is approximately ??.

$p_{11} = (47881607223.002250, 34039.066160)$
$p_{33} = (37362983980.381652, 223305.323451)$
$p_{55} = (10239564921.821903, 0.0)$
$p_{66} = (10239564921.827581, 0.0)$
$p_{13} = (13930827662.989664, 10086.232336)$

Figure 1 shows the polar representation of phase velocities of qP, qSV and SH waves of the dry core at 1 MHz. Anisotropy is clearly observed in the behavior of the velocities of the three wave modes.

Phase velocities and attenuation using using hydrocarbon saturated samples

This subsection considers the same sample of the previous experiment, but with the two periodic layers saturated by 100 % oil. '11' and '33' waves phase velocities as function of frequency are shown in Figure2. The corresponding attenuation factors $1000/Q_{11}$ and $1000/Q_{33}$ are displayed in Figure 3.

Note that the attenuation peak for '33' waves is shifted to higher frequencies as compared with '11' waves. This is also observed in Santos et al (2019).

Estimation of the stiffness tensor of dry rock core sample through numerical simulations based on rock physics

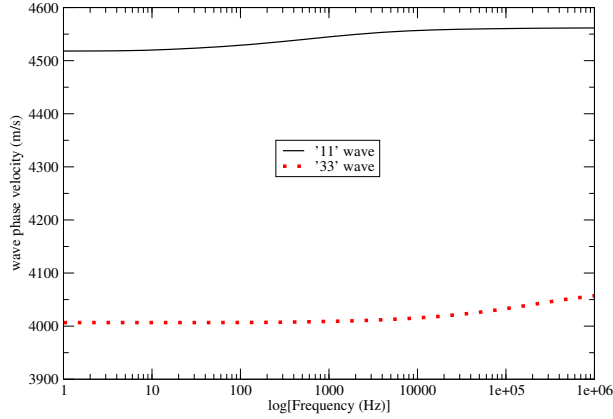


Figure 3: Wave phase velocity as function of frequency for '11' and '33' waves. The medium consists of a periodic sequence of seventy nine layers of the composite porous solid including 23 % of kerogen as a mineral and one kerogen layer. The pore space in both Materials is saturated with 100 % oil.

ACKNOWLEDGMENTS

We would like to thank Pluspetrol S.A. and Solaer Ingeniería S.A. for providing us with the measured data.

APPENDIX A

Following Gelinsky and Shapiro (1997), the relaxed stiffnesses are given by the expressions

$$\begin{aligned}
 c_{66}^r &= \langle \mu \rangle, \\
 c_{11}^r - 2c_{66}^r &= c_{12}^r = 2 \left\langle \frac{\lambda_m \mu}{E_m} \right\rangle + \left\langle \frac{\lambda_m}{E_m} \right\rangle^2 \left\langle \frac{1}{E_m} \right\rangle^{-1} \\
 &\quad + \frac{B_6^{*2}}{B_8^*}, \\
 c_{13}^r &= \left\langle \frac{\lambda_m}{E_m} \right\rangle \left\langle \frac{1}{E_m} \right\rangle^{-1} + \frac{B_6^* B_7^*}{B_8^*}, \\
 c_{33}^r &= \left[\left\langle \frac{1}{E_m} \right\rangle - \left\langle \frac{\alpha}{E_m} \right\rangle^2 \left\langle \frac{E_G}{ME_m} \right\rangle^{-1} \right]^{-1}, \\
 c_{55}^r &= \langle \mu^{-1} \rangle^{-1}, \\
 B_6^* &= -B_8^* \left(2 \left\langle \frac{\alpha \mu}{E_m} \right\rangle + \left\langle \frac{\alpha}{E_m} \right\rangle \left\langle \frac{\lambda_m}{E_m} \right\rangle \left\langle \frac{1}{E_m} \right\rangle^{-1} \right), \\
 B_7^* &= -B_8^* \left\langle \frac{\alpha}{E_m} \right\rangle \left\langle \frac{1}{E_m} \right\rangle^{-1}, \\
 B_8^* &= \left[\left\langle \frac{1}{M} \right\rangle + \left\langle \frac{\alpha^2}{E_m} \right\rangle - \left\langle \frac{\alpha}{E_m} \right\rangle^2 \left\langle \frac{1}{E_m} \right\rangle^{-1} \right]^{-1},
 \end{aligned} \tag{A-1}$$

where $\langle \cdot \rangle$ means weighted average between layers.

When there is no interlayer flow (unrelaxed regime), the coef-

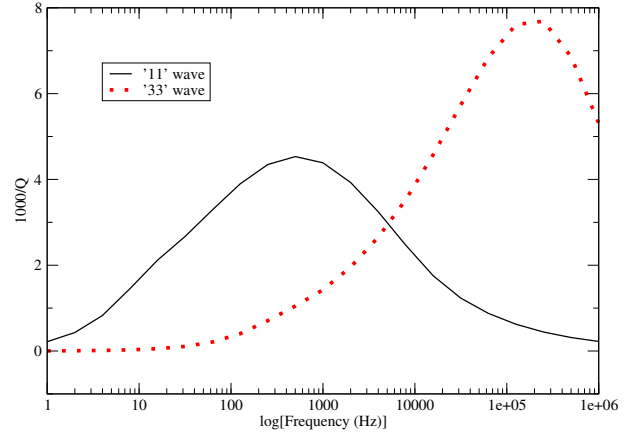


Figure 4: Attenuation factor 1000/Q as function of frequency for '11' and '33' waves. The medium consists of a periodic sequence of seventy nine layers of a composite porous solid including 23 % of kerogen as a mineral and one dry kerogen layer. The pore space in both Materials is saturated with 100 % oil.

ficients are (Gelinsky and Shapiro, 1997),

$$\begin{aligned}
 c_{66} &= c_{66}^r, \\
 c_{11} - 2c_{66} &= c_{12} = 2 \left\langle \frac{(E_G - 2\mu)\mu}{E_G} \right\rangle + \left\langle \frac{E_G - 2\mu}{E_G} \right\rangle^2 \left\langle \frac{1}{E_G} \right\rangle^{-1}, \\
 c_{13} &= \left\langle \frac{E_G - 2\mu}{E_G} \right\rangle \left\langle \frac{1}{E_G} \right\rangle^{-1}, \\
 c_{33} &= \left\langle \frac{1}{E_G} \right\rangle^{-1}, \quad c_{55} = c_{55}^r.
 \end{aligned} \tag{A-2}$$

REFERENCES

- J. M. Carcione and S. Picotti, P-wave seismic attenuation by slow-wave diffusion, Effects of inhomogeneous rock properties, *Geophysics* 71 (2006) O1-O8.
- Jose M. Carcione, Hans B. Helle, Juan E. Santos and Claudia L. Ravazzoli, A constitutive equation and generalized Gassmann modulus for multimineral porous media, *Geophysics*, 70 (2); doi: 10.1190/1.1897035
- S. Gelinsky and S. A. Shapiro, Poroelastic Backus-averaging for anisotropic, layered fluid and gas saturated sediments, *Geophysics* 62 (1997) 1867-1878.
- González Celis, R. et al. (2020) Matriz energética mundial y el cambio climático: Estado actual. *Master Thesis - Gestión Sostenible de la Energía*.
- Grechka, V. and Tsvankin, I. (2003) Feasibility of seismic characterization of multiple fracture sets. *Geophysics*, **68**, 1399–1407.
- F. Krzikalla and T. M. Müller, Anisotropic P-SV-wave dispersion and attenuation due to interlayer flow in thinly layered

Estimation of the stiffness tensor of dry rock core sample through numerical simulations based on rock physics

porous rocks, *Geophysics* 76 W 135 (2011); doi:10.1190/1.3555077.

J.E. Santos, G.B. Savioli, J. M. Carcione and J. Ba, Effect of capillarity and relative permeability on Q anisotropy of hydrocarbon source rocks, *Geophys. J. Int.* (2019) 218, 1199–1209, doi: 10.1093/gji/ggz217.

J. E. White, N. G. Mikhaylova and F. M. Lyakhovitskiy, Low-frequency seismic waves in fluid saturated layered rocks, *Physics of the Solid Earth* 11 (1975) 654-659.